CHEMISTRY OF MATERIALS

ARTICLE

pubs.acs.org/cm

Catechol Redox Induced Formation of Metal Core−Polymer Shell Nanoparticles

Kvar C. L. Black,[†,∥] Zhongqiang Liu,[†,∥] and Phillip B. Messersmith*[,†,‡,§,∥,⊥,#]

[†]Biomedical Engineering Department, [‡]Materials Science and Engineering Department, [§]Chemical and Biological Engineering Department, [∥]Chemistry of Life Processes Institute, [⊥]Institute for Bionanotechnology in Medicine, and [#]Robert H. Lurie Comprehensive Cancer Center, Northwestern University, Evanston, Illinois 60208, United States

Supporting Information

ABSTRACT: A novel strategy was developed to synthesize polymer-coated metal nanoparticles (NPs) through reduction of metal cations with 3,4-dihydroxyphenylalanine (DOPA)-containing poly(ethylene glycol) (PEG) polymers. Catechol redox chemistry was used to both synthesize metal NPs and simultaneously form a cross-linked shell of PEG polymers on their surfaces. DOPA reduced gold and silver cations into neutral metal atoms, producing reactive quinones that covalently cross-linked the PEG molecules around the surface of the NP. Importantly, these PEG-functionalized metal NPs were stable in physiological ionic strengths and under centrifugation and hold broad appeal since they absorb and scatter light in aqueous solutions.

KEYWORDS: catechol, quinone, gold, silver, nanoparticle, plasmon, cross-link

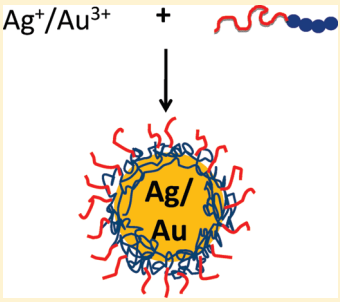

INTRODUCTION

Catechol-containing molecules serve diverse functions in nature including surface adhesion,[1,2] photoprotection,[3] and neuromodulation,[4] reflecting a chemical versatility that includes coordination of metal ions[5] in solution, formation of π-electron[6] and hydrogen bond[7] interactions, and redox activity.[8] At solid interfaces, catechols employ one or more of these interactions to form robust adhesion. An example is given by 3,4-dihydroxyphenylalanine (DOPA), which plays a strong role in mussel foot protein adhesion.[9−12] DOPA residues are believed to be essential in the solidification of the adhesive during attachment through oxidative cross-linking[1] and may also participate in interfacial adhesion.[13] This versatile chemical repertoire confers upon catechol-containing molecules the ability to adhere to almost any material of either organic or inorganic origin.[14]

Noble metal nanoparticles (NPs) composed of gold and silver hold broad appeal in optical applications due to their unique dielectric properties associated with the surface plasmon resonance that interacts strongly with electromagnetic radiation near the plasma frequency.[15] The optical properties can be tuned by size, shape, and composition of the metal at the nanoscale,[16] and metal NPs can be integrated into aqueous environments when functionalized with polymers such as poly(ethylene glycol) (PEG).[17−19] Redox reactions are commonly used to form metal NPs in solution with reducing agents such as citric acid and ascorbic acid.[20−22] Hydroxylated aromatics such as hydroquinone[23−26] and tyrosine-containing peptides were used to form silver[27,28] and platinum[29] NPs and were selected in silver-binding phage display.[30] Catechol-containing molecules form metal NPs[31,32] and hold additional advantages in forming robust interfaces between metal surfaces and organic molecules compared to other structures, including the ability to coordinate strongly to metals through two adjacent hydroxyls and covalently cross-link when oxidized to quinones by Michael addition and Schiff base reactions. In this study, DOPA-containing PEG polymers induced spontaneous formation of PEG-coated gold and silver NPs from metal salts. A unique feature of the reported approach is the redox coupling of metal reduction with catechol oxidation and simultaneous polymerization to yield a stable cross-linked polymer shell on the NP surface.

MATERIALS

Fmoc-DOPA(Acetonide)-OH and 2-chlorotrityl chloride resin were purchased from EMD Chemicals (Novabiochem, Gibbstown, NJ); methoxy-poly(ethylene glycol) amine (mPEG-NH_2, M_n = 1937 g/mol) was purchased from Sunbio Corporation (Korea); *N*,*N*-diisopropylethylamine (DIPEA), dichloromethane (DCM), methanol (MeOH), piperidine, *N*-methyl-2-pyrrolidone (NMP), benzotriazol-1-yloxytris-(dimethylamino)-phosphonium hexafluorophosphate (BOP), acetic anhydride (Ac_2O), triflouroacetic acid (TFA), toluene, dimethylformamide (DMF), gold chloride ($HAuCl_4$), silver nitrate ($AgNO_3$), sodium chloride (NaCl), 2,5-dihydroxybenzoic acid (DBA), sodium phosphate, glycine, and bicine were purchased from Sigma-Aldrich, Inc. (St. Louis, MO); TRIS hydrochloride was purchased from J.T. Baker (Phillipsburg, NJ); and TRIS base was purchased from Thermo Fisher Scientific (Waltham, MA).

Received: August 25, 2010
Revised: December 14, 2010
Published: January 18, 2011

ACS Publications © 2011 American Chemical Society

dx.doi.org/10.1021/cm1024487 | *Chem. Mater.* 2011, 23, 1130–1135

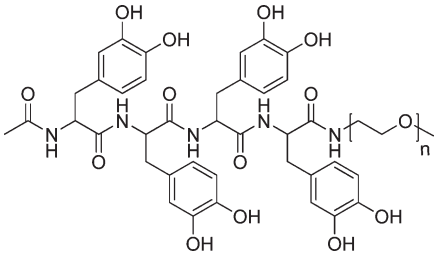

Figure 1. Molecular structure of Ac-DOPA$_4$-mPEG polymer.

METHODS

Synthesis of Ac-[DOPA(Acetonide)]$_4$-OH Peptide. The protected tetrapeptide acid was synthesized on 2-chlorotrityl chloride resin using a standard Fmoc-based solid phase peptide synthesis strategy. To introduce the first amino acid, Fmoc-DOPA(Acetonide)-OH (1 mmol) and DIPEA (4 mmol) were dissolved in 15 mL of DCM and shaken with 2-chlorotrityl chloride resin (1.6 g, 1.6 mmol) for 4 h. After washing, the resin was capped with methanol using DCM/MeOH/DIPEA (17:2:1). Fmoc was removed by 20% piperidine in NMP. Subsequent amino acid additions were performed using Fmoc-DOPA(Acetonide)-OH/BOP/DIPEA (1.5 mmol each) in the minimum amount of NMP. A ninhydrin test was performed after each amino acid addition to monitor the coupling result. After removal of the Fmoc group of the fourth amino acid, the tetrapeptide was capped with an acetyl group using Ac_2O/DIPEA/NMP (1:4:40). The protected peptide acid was cleaved from the resin using 2% TFA in DCM solution. MALDI-TOF (negative mode) yielded a monoisotopic mass $[M - H]^-$ of 935.71, matching the theoretical mass of 935.37 (Supporting Information Figure S1a).

Synthesis of Ac-DOPA$_4$-mPEG. mPEG-NH_2 (0.44 g) was azeotropically dried with toluene and stirred with Ac-[DOPA(Acetonide)]$_4$-OH (0.37 g), BOP (0.32 g), and DIPEA (0.136 mL) in dry DCM (3 mL) for two days. The polymer was precipitated with cold dry ethyl ether, dissolved in MeOH, and precipitated again with ether. The precipitate was dissolved in water, centrifuged, and filtered. The clear filtrate was lyophilized into a white powder. MALDI-TOF (positive mode) revealed a group of peaks centered at 2865.84 m/z. The content of DOPA was determined using UV−vis spectroscopy. Taking Ac-[DOPA-(Acetonide)]$_4$-OH peptide as standard, a correlation was established between the concentrations of the peptide in DMF and the absorption intensities at 289 nm. The UV absorption of Ac-[DOPA(Acetonide)]$_4$-mPEG was measured, and the degree of modification was calculated to be 93%. The synthesized Ac-[DOPA(Acetonide)]$_4$-mPEG (20 mg) was stirred in 2 mL of TFA/MeOH/water/DCM (30: 2.5: 2.5: 65) for 3 h to give Ac-DOPA$_4$-mPEG (Figure 1). The deprotected catechol structure was characterized with MALDI-TOF (positive mode); a group of peaks centered at 2705.93 was confirmed (Supporting Information Figure S1b).

Metal NP Synthesis. In one series of experiments, 1 mL aliquots of 370 μM Ac-DOPA$_4$-mPEG in ultrapure deionized water were prepared, and the pH was adjusted (6.0−9.0) with the addition of small volumes of 1 M NaOH. Then 107 μM metal salt ($HAuCl_4$ or $AgNO_3$) was added to each aliquot. In another series, with and without the presence of 10 mM TRIS buffer, varying concentrations of metal salt solution (50−3000 μM) were added to aliquots of 370 μM Ac-DOPA$_4$-mPEG at pH 8.5 and mixed vigorously. Identical experiments were performed with 123 μM Ac-DOPA$_4$-mPEG solutions.

Optical Spectroscopy. Time-dependent spectra of 123 μM Ac-DOPA$_4$-mPEG solutions during gold and silver NP formation were acquired in a one beam Hewlett-Packard (Palo Alto, CA) 8452A diode array spectrophotometer over the 250−820 nm optical range and compared to a water blank. Spectra were immediately and continually acquired for the duration of the reaction, and scan times ranged between 0.1 and 0.5 s.

Electron Microscopy (EM). Metal NP samples were centrifuged at 9000 rpm for 10 min, and the supernatant solution was removed. 5−10 μL of the NP pellet was dropped onto an EM carbon grid (Electron Microscopy Sciences, Hatfield, PA) and allowed to dry overnight. For samples stained with phosphotungstic acid, grids with dried metal NPs were dipped in a 10% solution for 5 min and then dipped in a solution of deionized water three times, soaked for 30 s, and allowed to dry. Transmission EM (TEM), Z-contrast (ZC) EM (a mode that provides bright contrast to high atomic number elements), secondary EM (SEM), and electron diffraction imaging were performed on a Hitachi HD-2300 Ultra High Resolution FE-STEM.

RESULTS

Addition of gold chloride into a basic solution of Ac-DOPA$_4$-mPEG (Figure 1) induced a red color change in the solution that darkened over the span of a minute (Figure 2a, inset, and Supporting Information Figure S2a). To characterize this color transformation, optical spectroscopy was performed before and after the addition of gold chloride into PEG solutions (Figure 2a). Before gold addition, a lone 280 nm DOPA absorption peak was detected. Ten seconds after addition of $HAuCl_4$, a 390 nm peak and a 550 nm peak formed, and within 1 min the 390 and 550 nm peak intensities stabilized.

A series of experiments were performed in which the concentration of gold chloride was varied (107 μM − 1970 μM) under constant polymer concentration (Table 1). A red color change occurred in samples with gold concentrations less than 1000 μM, whose optical spectra contained both a transient 390 nm peak and a stable peak centered between 525 and 560 nm. The 525−560 nm peak broadened, and the center wavelength red-shifted with increasing amounts of gold up to 1000 μM. Importantly, when 1970 μM gold chloride was added to 370 μM polymer solutions, no red color change or absorbance at 525−560 nm was observed, and the sample remained similar in appearance to the yellow color of pure gold chloride solution (Supporting Information Figure S2b). Experiments were also performed in the presence of TRIS buffer at 8.5 pH and yielded qualitatively similar color changes and optical spectra as their unbuffered counterparts (Supporting Information Figure S3).

To confirm the formation of gold NPs, samples were imaged with electron microscopy. In all samples with visible absorbance in the 525−560 nm range, sub-80 nm NPs were evident. Additionally, control over gold NP size between 10 and 70 nm was achieved by varying the concentration of gold chloride between 107 μM and 625 μM in 370 μM polymeric solutions (1480 μM catechol). Table 1 lists the polymer and metal ion concentrations and the resulting plasmon center wavelength and particle size. Micrographs of 70 nm gold NPs are shown in Figure 2. High resolution imaging under TE mode of a single NP provided evidence of a metal core and a less electron dense coating 9.4 nm thick (Figure 2b), SEM provided NP surface morphology of the metal core (Figure 2b, inset), and EDS spectral imaging confirmed that gold was localized to the core (data not shown). Electron diffraction was performed on the gold core of single NPs (Supporting Information Figure S4),and gave evidence of polycrystalline features including twinning doublets and crystal orientation changes. Furthermore, multimode electron microscopy was performed on a group of gold NPs that appeared as closely packed spheres under SEM (Figure 2c).

dx.doi.org/10.1021/cm1024487 |*Chem. Mater.* 2011, 23, 1130–1135

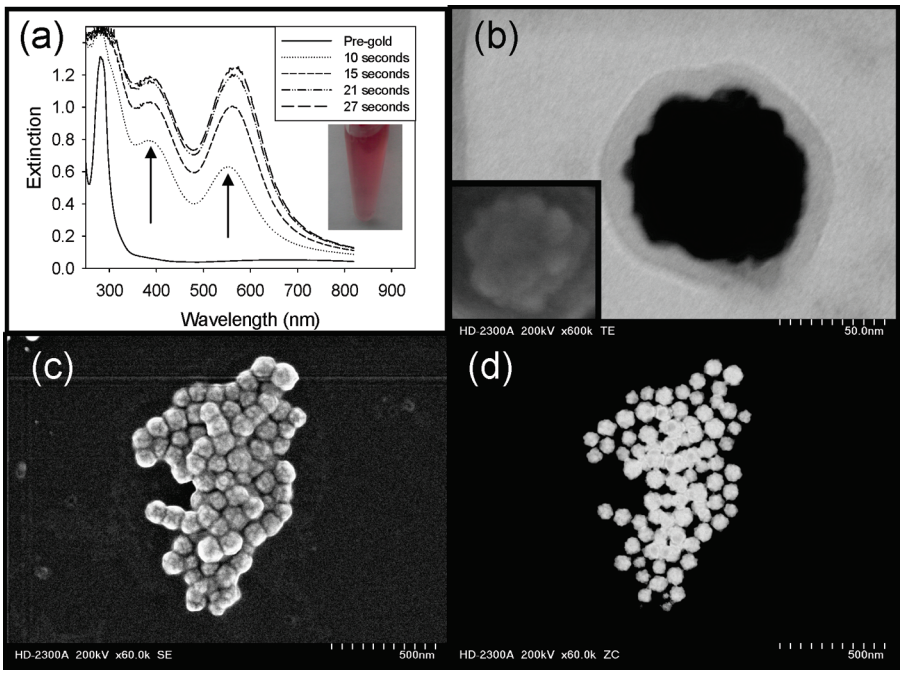

Figure 2. Spontaneous formation of Ac-DOPA$_4$-mPEG-coated gold nanoparticles: (a) UV−vis extinction curves at successive time points after mixing 102 μM $HAuCl_4$ with 123 μM Ac-DOPA$_4$-mPEG. The inset shows a photograph of the suspension after 1 h. (b−d) EM of gold NPs formed with Ac-DOPA$_4$-mPEG: (b) TEM and SEM (inset) of a single gold NP, (c) SEM, and (d) Z-Contrast EM of a cluster of gold NPs.

Table 1. Table Representing the Concentration of Ac-DOPA$_4$-mPEG and Metal Salt, the Metal−DOPA Ratio, the Surface Plasmon Resonance (SPR) Center Wavelength, and the Nanoparticle Size Determined by TEM of Metal Nanoparticle Samples

[Ac-DOPA$_4$-mPEG] (μM)	[Au] (μM)	[Ag] (μM)	[M]/[DOPA]	SPR λ (nm)	size (nm)
370	107	0	0.0723	525	10.4 ± 6.7
370	427	0	0.289	547	38.7 ± 5.5
370	625	0	0.423	559	68 ± 18
370	1970	0	1.33	ND	N/A
370	0	107	0.0723	415	16.9 ± 2.4

Under Z-contrast imaging (Figure 2d), the same cluster of NPs was observed to be separated from each other by up to 20 nm. When cryo-TEM was performed on a sample of gold NPs formed with the DOPA-containing PEG polymers to characterize their dispersion in suspension, well-dispersed gold particles were observed (Supporting Information Figure S5).

To observe changes in polymer mass correlated to oxidation-induced polymerization, samples were plated at various times during the gold NP synthesis, and MALDI-TOF-MS was performed (see Supporting Information for methods). Prior to the addition of $HAuCl_4$, a distribution of peaks centered at 2749 m/z with spacing of 44 (the weight of a PEG monomer unit) between peaks was detected in all pH conditions, representing individual Ac-DOPA$_4$-mPEG molecules. No peak distributions at higher masses were detected. Likewise, when gold was added at pH 6 (where NP formation did not occur as indicated by spectroscopic analysis), signals from the Ac-DOPA$_4$-mPEG molecule were detected. However, under conditions where NP formation was observed (Table 1), in addition to individual Ac-DOPA$_4$-mPEG molecules, a distribution of peaks centered at twice the molecular weight of a single Ac-DOPA$_4$-mPEG molecule (5388 m/z) was detected (Supporting Information Figure S1c). XPS analysis of gold NPs revealed C 1s and O 1s peaks (Supporting Information Figure S6a), as well as weak peaks from Au 4f.

Similar results were obtained when silver nitrate was added to Ac-DOPA$_4$-mPEG using the same method as described with gold chloride. In basic conditions and excess catechol, a yellow color change (Figure 3a and Supporting Information Figures S2c and S3) resulting from a peak centered at ~410 nm occurred immediately after addition of $AgNO_3$, growing steadily for 1 min. TEM imaging of NPs from a sample with a 403 nm absorption maximum revealed NPs of 17 nm average size (Figure 3b), and XPS analysis of the same sample revealed C 1s, O 1s, Ag 2s, and Ag_2O peaks (Supporting Information Figure S6b).

To investigate their stability in saline conditions, gold and silver NPs formed with Ac-DOPA$_4$-mPEG were incubated in 100 mM sodium chloride; control gold NPs with a 520 nm peak coated with citrate were also evaluated. In the case of gold, the peak in the 525−560 nm range from Ac-DOPA$_4$-mPEG-stabilized NPs did not shift or change shape when placed in 100 mM saline solution for 24 h. In contrast, the peak of citrate-stabilized gold NPs broadened and red-shifted in 10 mM NaCl, further red-shifting and broadening with increasing concentrations of salt (Figure 4 and Supporting Information Figure S7a). The silver NP suspensions formed with Ac-DOPA$_4$-mPEG were also stable in 100 mM sodium chloride (Supporting Information Figure S7b).

dx.doi.org/10.1021/cm1024487 |*Chem. Mater.* 2011, 23, 1130–1135

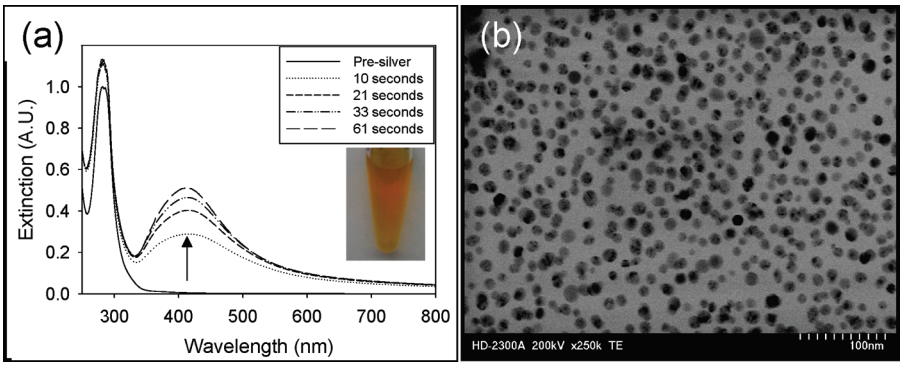

Figure 3. Spontaneous formation of Ac-DOPA$_4$-mPEG-coated silver nanoparticles: (a) UV−vis extinction curves at successive time points during the formation of silver NPs with Ac-DOPA$_4$-mPEG polymers. The inset shows a photograph of the suspension after 1 h. (b) TEM microscopy of silver NPs formed with Ac-DOPA$_4$-mPEG.

DISCUSSION

Covalent reactions resulting from oxidation of DOPA are believed to play an important role in solidification and structural cohesion in mussel adhesive proteins[2] and sandcastle worm cement[33−35] and are believed to proceed via oxidation of DOPA to quinone[9,36] followed by their reaction to form covalent di-DOPA cross-links.[37,38] In this study, coupling of catechol oxidation with reduction of metal ions was demonstrated as a simple and convenient route for in situ formation of metal NPs while also ensuring a robust interface between the metal surface and surface grafted polymers.

The addition of gold and silver salts into Ac-DOPA$_4$-mPEG solutions led to rapid color change consistent with the formation of Au and Ag NPs with plasmon resonances centered at 525−560 nm and 400−430 nm, respectively. NP formation was clearly linked to the oxidation of DOPA in the Ac-DOPA$_4$-mPEG polymer, as peaks typical of DOPA−quinone (390 nm) and the plasmon resonance co-evolved during the reaction (Figure 2a arrows). Control over particle size within the range 10−70 nm was achieved by manipulating the molar ratio of catechol to metal during reaction (Table 1). A general correlation between NP size and plasmon resonance was observed, with larger NPs giving rise to plasmon resonances at higher wavelengths, matching previous reports.[15,16] SEM analysis of 70 nm gold NPs provided evidence in support of clustering of smaller nanoparticles (Figure 2b, inset).

EM analysis of the NPs isolated from the reaction mixture showed that the reaction culminated in the formation of well-dispersed NPs (Supporting Information Figure S5) with a core−shell structure composed of a polycrystalline metal core (Supporting Information Figure S4) and an organic shell of thickness <10 nm (Figures 2 and 3). Once dried on an EM grid, SEM imaging that emphasizes the secondary electrons from the surface-bound PEG polymers revealed aggregates of NPs. However, Z-contrast imaging was used to accentuate the metal cores, revealing clear gaps between NP cores which presumably were occupied by Ac-DOPA$_4$-mPEG polymers comprising the NP shell. Metal core−polymer shell morphology was also detected by TEM with EDS spectral imaging (data not shown). The approximate thickness of the polymer shell (~9.4 nm) lies between the contour length (15.8 nm) and the dimensions of a tethered 2 kDa PEG chain (4.8 nm),[39] implying an extended conformation,[40] possibly due to dense polymer surface packing.

Evidence for covalent coupling of Ac-DOPA$_4$-mPEG was obtained through MALDI-MS analysis of the reaction mixture.

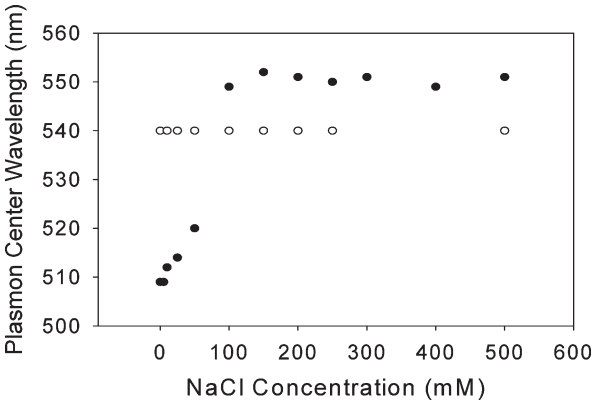

Figure 4. Plot of the visible extinction peak center wavelength from Ac-DOPA$_4$-mPEG-coated (white) and citrate-coated (black) gold nanoparticles as a function of sodium chloride concentration.

Higher molecular weight species were observed shortly after mixing polymer and metal salt, confirming Ac-DOPA$_4$-mPEG polymerization during NP formation. Detection of the Ac-DOPA$_4$-mPEG dimer by MALDI only occurred upon the addition of metal salt at pH 8.7, providing further evidence that quinone-mediated cross-linking of Ac-DOPA$_4$-mPEG was concurrent with metal NP formation. The most likely explanation for these observations is that metal reduction led to catechol oxidation and ultimately di-DOPA coupling of Ac-DOPA$_4$-mPEG polymers. Importantly, this study represents an alternative approach to previously reported methods[41,42] to form stable cross-linked polymer shells on NPs, one that is catalyzed by the same catechol redox reaction that causes the formation of the metal nanocrystals in situ.

Taken together, the presence of metal NP plasmon resonances, Au, Ag, ether C, and O peaks in XPS, as well as core−shell morphology evident in NPs under EM provide evidence of a PEG polymer coating on the metal NPs. The presence of a PEG shell should confer stability against aqueous aggregation of the NPs, particularly under high ionic strength conditions as would be observed in many biomedical applications of NPs. Indeed, Ac-DOPA$_4$-mPEG coated NPs were stable in high ionic strength solutions whereas citrate-stabilized Au NPs aggregated as evidenced by red shift of the surface plasmon absorbance (Figure 4 and Supporting Information Figure S7). The covalent cross-linking of grafted Ac-DOPA$_4$-mPEG polymers within the polymer shell, as well as the robust adhesion

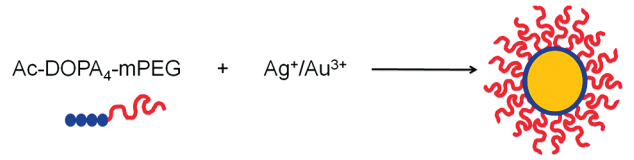

Figure 5. Schematic representing the addition of Ac-DOPA$_4$-mPEG with gold or silver ions to form a metallic NP core with a DOPA interface and a PEG shell.

afforded by DOPA at interfaces, should combine to create a robust core−shell NP, and in the future it may be possible to incorporate other DOPA-containing molecules into more complex and multifunctional assemblies such as biodegradable plasmonic liposomes.[43]

Our strategy builds upon recent work wherein catechol-containing molecules such as dopamine[14] or DOPA peptides[44] were used to graft polymers and biomolecules onto surfaces and represents an alternative approach to linking PEG and other polymers onto metal NP surfaces using polyamine,[17] thiol,[18] and thioctic acid[19] anchors. In contrast to these previous approaches, the catechol group of DOPA serves as metal reductant, molecular anchor, and polymerizable cross-linker, simultaneously inducing in situ metal NP formation while also providing a cohesively cross-linked and robust adhesive interface between the metal NP and the PEG polymer shell (Figure 5). Gold NPs between 10 and 70 nm were formed and stabilized with this strategy, the larger particles characterized by a cluster morphology coated in PEG that should provide electromagnetic hotspots between metal crystals for surface enhanced Raman spectroscopy (SERS).[45,46] Further, both gold and silver NPs were formed and stabilized, an important advantage for potential applications that use silver to either tune plasmonic absorption and scattering[47] or provide an antimicrobial therapeutic effect.[48] Through its molecular design that contains four DOPA residues per molecule and aided by further polymerization during metal NP formation, Ac-DOPA$_4$-mPEG is expected to lead to multivalent attachment onto the NP surface, as is hypothesized in the case of mussel adhesive proteins that contain multiple DOPA residues.[11,49,50] Although we do not know the exact nature of the chemical interaction between DOPA and the metal NP surface, charge transfer and physisorption interactions from the aromatic side chain of DOPA[6] and coordination through the catechol oxygen atoms[51] have been hypothesized.

CONCLUSIONS

A catechol redox based strategy was employed to induce spontaneous in situ formation of polymer-coated gold and silver NPs from mixtures of a DOPA-containing polymer and noble metal salts. In this biomimetic strategy the catechol side chain of DOPA serves multiple roles: as a reducing agent for metal ions; as an anchoring chemistry for multivalent binding of the polymer onto the NP surface; and as a chemical precursor for cross-linking of the polymer shell. The resulting core−shell NPs exhibit plasmon resonance behavior characteristic of noble metal NPs and are stable toward aggregation in ionic aqueous media. Potentially, this biomimetic strategy can be used to produce surface derivatized metal NPs for diagnostic and therapeutic applications.

ASSOCIATED CONTENT

Supporting Information. Additional results including MALDI-TOF-MS, color images, optical spectroscopy, electron diffraction, cryo-TEM, and XPS of nanoparticle solutions (PDF). This material is available free of charge via the Internet at http://pubs.acs.org.

AUTHOR INFORMATION

Corresponding Author

*Biomedical Engineering Department, Northwestern University, 2145 Sheridan Road, Evanston, IL 60208. Phone: (847) 467-5273. Fax: (847) 491-4928. E-mail:philm@northwestern.edu.

ACKNOWLEDGMENT

The work was supported by National Institutes of Health (NIH) Grant R37 DE014193. K.C.L.B. was partly supported by a NIH Health Ruth Kirschstein NRSA fellowship from the National Institute of Dental and Craniofacial Research (F31 DE019750). The content is solely the responsibility of the authors and does not necessarily represent the official views of the National Institute of Dental and Craniofacial Research or the National Institutes of Health. The authors also acknowledge the NUANCE, Keck II, and IMSERC facilities at Northwestern University for their TEM, UV−vis, and MALDI-TOF-MS instruments, respectively, and Jinsong Wu of NUANCE for acquiring the cryo-TEM images.

REFERENCES

(1) Waite, J. H. *Int. J. Adhes. Adhes.* **1987**, *7*, 9–14.
(2) Waite, J. H. *Integr. Comp. Biol.* **2002**, *42*, 1172–1180.
(3) Brenner, M.; Hearing, V. J. *Photochem. Photobiol.* **2008**, *84*, 539–549.
(4) Callier, S.; Snapyan, M.; Crom, S. L.; Prou, D.; Vincent, J.-D.; Vernier, P. *Biol. Cell* **2003**, *95*, 489–502.
(5) Pierpont, C. G.; Buchanan, R. M. *Coord. Chem. Rev.* **1981**, *38*, 45–87.
(6) Weinhold, M.; Soubatch, S.; Temirov, R.; Rohlfing, M.; Jastorff, B.; Tautz, F. S.; Doose, C. *J. Phys. Chem. B* **2006**, *110*, 23756–23769.
(7) Burzio, L. A.; Waite, J. H. *Protein Sci.* **2001**, *10*, 735–740.
(8) Uchimiya, M.; Stone, A. T. *Geochim. Cosmochim. Acta* **2006**, *70*, 1388–1401.
(9) Yu, M.; Hwang, J.; Deming, T. J. *J. Am. Chem. Soc.* **1999**, *121*, 5825–5826.
(10) Suci, P. A.; Geesey, G. G. *Colloids Surf., B* **2001**, *22*, 159–168.
(11) Waite, J. H.; Qin, X. *Biochemistry* **2001**, *40*, 2887–2893.
(12) Waite, J. H. *J. Biol. Chem.* **1983**, *258* (5), 2911–2915.
(13) Lee, H.; Scherer, N. F.; Messersmith, P. B. *Proc. Natl. Acad. Sci. U.S.A.* **2006**, *103* (35), 12999–13003.
(14) Lee, H.; Dellatore, S. M.; Miller, W. M.; Messersmith, P. B. *Science* **2007**, *318*, 426–430.
(15) Simmons, J. H.; Potter, K. S. *Optical Materials*; Academic Press: San Diego, 2000.
(16) Jain, P. K.; Lee, K. S.; El-Sayed, I. H.; El-Sayed, M. A. *J. Phys. Chem. B* **2006**, *110*, 7238–7248.
(17) Miyamoto, D.; Oishi, M.; Kojima, K.; Yoshimoto, K.; Nagasaki, Y. *Langmuir* **2008**, *24* (9), 5010–5017.
(18) Duchesne, L.; Gentili, D.; Comes-Franchini, M.; Fernig, D. G. *Langmuir* **2008**, *24*, 13572–13580.
(19) Zhang, G.; Yang, Z.; Lu, W.; Zhang, R.; Huang, Q.; Tian, M.; Li, L.; Liang, D.; Li, C. *Biomaterials* **2009**, *30*, 1928–1936.
(20) Turkevich, J.; Stevenson, P. C.; Hillier, J. *Discuss. Faraday Soc.* **1951**, *11*, 55.
(21) Kimling, J.; Maier, M.; Okenve, B.; Kotaidis, V.; Ballot, H.; Plech, A. *J. Phys. Chem. B* **2006**, *110* (32), 15700–15707.
(22) Enustun, B. V.; Turkevich, J. *J. Am. Chem. Soc.* **1963**, *85*, 3317.
(23) Yi, H.-B.; Diefenbach, M.; Choi, Y. C.; Lee, E. C.; Lee, H. M.; Hong, B. H.; Kim, K. S. *Chem.—Eur. J.* **2006**, *12*, 4885–4892.

(24) Perez, M. A.; Moiraghi, R.; Coronado, E. A.; Macagno, V. A. *Cryst. Growth Des.* **2008**, *8* (4), 1377–1383.
(25) Gentry, S. T.; Fredericks, S. J.; Krchnavec, R. *Langmuir* **2009**, *25*, 2613–2621.
(26) Perrault, S. D.; Chen, W. C. W. *J. Am. Chem. Soc.* **2009**, *131*, 17042–17043.
(27) Jacob, J. A.; Mahal, H. S.; Biswas, N.; Mukherjee, T.; Kapoor, S. *Langmuir* **2007**, *24* (2), 528–533.
(28) Xie, J.; Lee, J.-Y.; Wang, D. I. C.; Ting, Y. P. *ACS Nano* **2008**, *1* (5), 429–439.
(29) Li, Y.; Whyburn, G.; Huang, Y. *J. Am. Chem. Soc.* **2009**, *131* (44), 15998–15999.
(30) Naik, R. R.; Stringer, S. J.; Agarwal, G.; Jones, S. E.; Stone, M. O. *Nat. Mater.* **2002**, *1*, 169–172.
(31) Baron, R.; Zayats, M.; Willner, I. *Anal. Chem.* **2005**, *77*, 1566–1571.
(32) Begum, N.; Mondal, S.; Basu, S.; Laskar, R.; Mandal, D. *Colloids Surf., B* **2009**, *71*, 113–118.
(33) Stewart, R. J.; Weaver, J. C.; Morse, D. E.; Waite, J. H. *J. Exp. Biol.* **2004**, *207*, 4727–4734.
(34) Endrizzi, B. J.; Huang, G.; Kiser, P. F.; Stewart, R. J. *Langmuir* **2006**, *22*, 11305–11310.
(35) Shao, H.; Bachus, K. N.; Stewart, R. J.; Water-Borne, A. *Macromol. Biosci.* **2009**, *9* (5), 464–471.
(36) Burzio, L. A.; Waite, J. H. *Biochemistry* **2000**, *39*, 11147–11153.
(37) Schonhorn, H. *Adhesion and adhesives: Interactions at interfaces*; Plenum: New York, 1981.
(38) McDowell, L. M.; Burzio, L. A.; Waite, J. H.; Schaefer, J. *J. Biol. Chem.* **1999**, *274* (29), 20293–20295.
(39) Moore, N. W.; Kuhl, T. L. *Biophys. J.* **2006**, *91* (5), 1675–1687.
(40) Jeppesen, C.; Wong, J. Y.; Kuhl, T. L.; Israelachvili, J. N.; Mullah, N.; Zalipsky, S.; Marques, C. M. *Science* **2001**, *293*, 465–468.
(41) Gittins, D. I.; Caruso, F. *Adv. Mater.* **2000**, *12* (24), 1947–1949.
(42) Joralemon, M. J.; O'Reilly, R. K.; Hawker, C. J.; Wooley, K. L. *J. Am. Chem. Soc.* **2005**, *127*, 16892–16899.
(43) Troutman, T. S.; Barton, J. K.; Romanowski, M. *Adv. Mater.* **2008**, *20*, 2604–2608.
(44) Dalsin, J. L.; Hu, B.-H.; Lee, B. P.; Messersmith, P. B. *J. Am. Chem. Soc.* **2003**, *125*, 4253–4258.
(45) Moskovits, M. *J. Raman Spectrosc.* **2005**, *36*, 485–496.
(46) Camden, J. P.; Dieringer, J. A.; Wang, Y.; Masiello, D. J.; Marks, L. D.; Schatz, G. C.; Duyne, R. P. V. *J. Am. Chem. Soc.* **2008**, *130*, 12616–12617.
(47) Link, S.; Wang, Z. L.; El-Sayed, M. A. *J. Phys. Chem. B* **1999**, *103*, 3529–3533.
(48) Rai, M.; Yadav, A.; Gade, A. *Biotechnol. Adv.* **2009**, *27*, 76–83.
(49) Waite, J. H. *J. Biol. Chem.* **1983**, *258* (5), 2911–2915.
(50) Papov, V. V.; Diamond, T. V.; Biemann, K.; Waite, J. H. *J. Biol. Chem.* **1995**, *270* (34), 20183–20192.
(51) Ooka, A. A.; Garrell, R. L. *Biopolymers* **2000**, *57*, 92–102.